Photoinduced Reactions in Polymerized Microemulsions[1]

S. Atik and J. K. Thomas*

Contribution from the Department of Chemistry, University of Notre Dame, Notre Dame, Indiana 46556. *Received October 15, 1982*

Abstract: Polymerized microemulsions with styrene cores are designed with either cetyltrimethylammonium bromide, CTAB, or cetylpyridinium chloride, CPC, surfaces. The nature of the styrene polymer core resembles more nearly that of a polystyrene film rather than polystyrene in solution. With CPC systems probe molecules such as pyrene only fluoresce in the rigid core of the particle; pyrene in the surface region is quenched very rapidly by CPC. Hence energy transfer and e^- transfer reactions involving pyrene can be studied exclusively in the core. Material diffusion is not important in these reactions, and energy transfer takes place via a Förster mechanism, while e^- transfer takes place via tunneling.

Introduction

In two previous publications,[2,3] we have described the various methods by which we have prepared polymerized microemulsions PμE, of styrene cross-linked with divinylbenzene in a cetyltrimethylammonium bromide CTAB, hexanol, oil in water microemulsion. It was found that various special properties were associated with these systems that made them attractive for use in photochemical studies. In particular, two sites were identified for a fluorescent probe molecule in the rigid polymerized core and in the much less rigid surfactant skin of the particle. As expected, the two sites behaved quite differently with regard to photoinduced reactions.

The present paper deals with further investigations of the systems, in particular with respect to several photoinduced reactions in the core of the particle. To this end another microemulsion incorporating cetylpyridinium chloride, CPC, in place of CTAB, was constructed and its properties are also reported. Fluorescence of probe molecules in the surfactant region of this system is completely quenched by the pyridinium group, while probes located in the polymerized core are unaffected. This enables us to focus directly on reactions of excited probes located only in the particle core.

Experimental Section

The experimental details are similar to those described in previous publications.[2-5]

Preparation and Polymerization of (O/W) Cetylpyridinium Chloride Microemulsion (CPC-μE). An oil in water μE composed of 1.0 g of CPC, 0.5 g of hexanol, and 1.0 g of 50% styrene–divinylbenzene in 50 mL of water was carefully prepared by slowly adding the water to a stirred mixture of the other components to yield a slightly bluish clear solution. A 0.1% solution (w/w) of initiater AIBN (based on monomer) was then solubilized in the system followed by removal of O_2 (by gentle N_2 bubbling for 5 min), and finally the system was heated in an oil bath (50 °C) until complete polymerization was achieved as determined spectrophotometrically. Proper dilution with water was then made to give a 0.01 M CPC–P-μE solution; P-μE indicates polymerized microemulsion.

The size of the P-μE particles was determined by dynamic light scattering by use of a Nicomp particle analyzer. The Nicomp particle analyzer is a light (single-mode 6328-A He–Ne laser) scattering computerized instrument which utilizes the theory of Rayleigh scattering of translational Brownian particles to compute the mean translation diffusion constant D. This is then used to determine the average hydrodynamic radius R using the Stokes–Einstein relationship for spherical particles, $D = kT/6\pi\eta R$.

A built-in microcomputer system performs rapid quadratic least-squares fit to the data, yielding D, R, σ (normalized standard deviation of the intensity-weighted distribution of diffusion constants), and χ-squares goodness of fit. A typical result obtained for 1.0×10^{-3} M CPC–P-μE is $D = 1.20 \times 10^{-7}$ cm^2/s; $R = 170$ Å; $\sigma = 0.50$, $\chi = 2.20$.

Materials. Styrene (Eastman) and divinylbenzene (Polyscience) were purified prior to use by removal of inhibitor by multiple washes with 5% sodium hydroxide solution followed by multiple-distilled water washes and finally vacuum distillation. Cetylpyridinium chloride (CPC) (Eastman), pyrene (Aldrich), pyrenebutyric acid (PBA) (Pfaltz and Bauer), and pyrenedodecanoic acid (PDA) were used as supplied.

Fluorescence spectra were measured on a Perkin-Elmer MPF 44 spectrofluorimeter. Laser flash photolysis studies were carried out using a Lambda Physik N_2 laser ($\lambda = 3371$ Å; pulse width = 6 ns; energy = 0.01 J) as an excitation source, and a Tektronix 7912 AD transient capture device to monitor the short-lived species formed. Data analysis was carried out on a Tektronix 4051 computer. A nitromite laser (PRA Co) with a pulse width of 200 ps was used for some of the work. The manufacturer's pulse width is stated to be 120 ps. We determined a width of 200 ps in our system, the detection being made with an ITT 4014 photodiode and a Tektronix 152 sampling system; the system rise time is 60 ps.

Results and Discussion

Spectroscopic Studies of PμE. Absorption and emission spectroscopy, as well as ^{13}C NMR studies are utilized to provide insight into the nature of the polymerized core of the PμE particles.

Polystyrene Core. The UV absorption spectrum of 0.01 M CTAB–PμE and CPC–PμE was found to be very similar to that of 0.01 M polystyrene in cyclohexane solution. However, the polystyrene emission spectrum in the PμE, shown in Figure 1b exhibits only excimer emission with λ_{max} 325 mn. This contrasts with a polystyrene/cyclohexane solution, Figure 1a, which exhibits appreciable monomer emission at λ_{max} 285 mn (Figure 1), as well as excimer emission. On the other hand, polystyrene film, Figure 1c, shows only excimer emission as in the PμE case. The data for polystyrene in solution and in the film form agree with other independent measurements.[6] Hence, it is reasonable to conclude that the polystyrene in the PμE takes the form obtained in a compact film, rather than a loosely cooled polymer in solution.

^{13}C NMR measurements of the CTAB–styrene–hexanol–D_2O and CPC–styrene–hexanol–D_2O systems prior to polymerization show lines typical of the various components of the system and are in agreement with those published in microemulsions.[7] The data show a partitioning of the hexanol co-surfactant between the core and interface of the assembly, as indicated previously.[7] Polymerization of the system to obtain a polymerized microemulsion directly changes the ^{13}C NMR spectrum, and signals characteristics of the α ^{13}C atom of hexanol and aromatic ^{13}C disappear. This is a consequence of the extremely high rigidity of the polymerized core of the PμE, which increases the spin–lattice relaxation time of the restricted ^{13}C signals, thus broadening the signal and placing them beyond detection.[8]

Quenching of the Fluorescence of P in CTAB- and CPC–P-μE. Previous fluorescence quenching studies[3] carried out in CTAB–P-μE showed that a probe molecule such as P is partitioned between the surfactant layer of CTAB and the polymerized latex particle. The mobility of P in the micellar surfactant region was

(1) The authors wish to thank the National Science Foundation for support of this work via grant No. CHE 82-01226.
(2) S. S. Atik and J. K. Thomas, *J. Am. Chem. Soc.*, **103**, 4279 (1981).
(3) S. S. Atik and J. K. Thomas, *J. Am. Chem. Soc.*, in press.
(4) S. S. Atik and J. K. Thomas, *J. Am. Chem. Soc.*, **103**, 3550 (1981).
(5) S. S. Atik and J. K. Thomas, *J. Am. Chem. Soc.*, **103**, 4367 (1981).
(6) M. C. Gupta, A. Gupta, J. Horwitz, and D. Kliger, *Macromolecules*, **15**, 1372 (1982).
(7) Y. Tricot, J. Kiwi, W. Niederberger, M. Grätzel, *J. Phys. Chem.*, **85**, 862 (1981).
(8) F. A. Bovey and T. K. Kwei, "Macromolecules", Academic Press, New York, 1979.

0002-7863/83/1505-4515$01.50/0

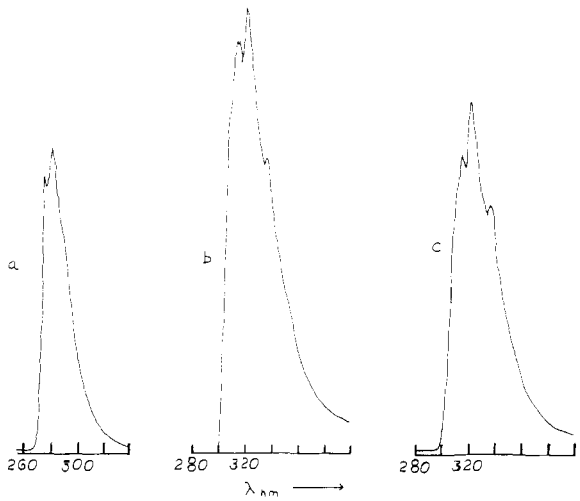

Figure 1. Fluorescence emission of (a) 10^{-2} M polystyrene in cyclohexane; (b) polymerized sytrene in CTAB–P-μE; and (c) polystyrene film excitation wavelength is 260 nm.

found to resemble that of micelles while the polymerized interior was found to be very rigid, and P solubilized in that region was found to be immobile and unquenchable by surface adsorbed quenchers such as I^- and CPC.

However, it is of interest to investigate the photophysical and photochemical reactions of P present exclusively in the polymerized phase. In order to eliminate complications arising from P located in the surfactant layer, a P-μE was prepared using CPC as surfactant instead of CTAB. Dynamic light scattering measurement yielded a radius of 170 Å for the CPC–P-μE particle, a value similar to that determined for CTAB–P-μE.[3] In this polymerized system, the pyridinium head groups of the surfactant region statically quench excited pyrene P* present in this region, leaving P* trapped in the polymer latex unaffected.[3] In an earlier study,[3] it was shown that CPC quenched pyrene fluorescence in a CTAB–P-μE. The quenching kinetics indicated that a portion of the pyrene fluorescence was quenched by CPC that associated with the CTAB–P-μE, where it efficiently quenched pyrene solubilized on the surfactant region of the particle. At higher CPC concentrations, micelles of CPC are formed and further quenching of the pyrene fluorescence is observed due to retraction of pyrene from CTAB–P-μE into CPC micelles where it is completely quenched. The partitioning of pyrene between CTAB–P-μE and CPC micelles was measured by analyzing the fluorescence quenching data.

Figure 2 compares the results of a fluorescence quenching study by using a CTAB–P-μE and CPC–P-μE, and using CPC as a quencher. The nonlinear Stern–Volmer plot for CTAB–P-μE is due to the existence of two sites for pyrene P: (a) the surfactant outer shell, where solubilized P would be mobile and free to diffuse to the surface to be dynamically quenched by the pyridinium head groups of CPC surfactants bound to the particle, and (b) the polymerized core, where trapped P would be effectively immobile within its excited state lifetime and therefore unquenchable by CPC.

The initial fast quenching is due to quenching of P* in the micellar site, and the later slower linear quenching is caused by the static quenching of P* solubilized in the CPC micelles in solution. From the slope of the linear portion of the quenching curve an equilibrium constant of 450 M^{-1} was derived for this partitioning process (as outlined earlier[3]), which can be described by the following equilibrium where M denotes micelles

$$MP \leftrightarrow M + P \qquad (1/K_m)$$

$$P + P\text{-}\mu E \leftrightarrow P\text{-}\mu E\cdot P \qquad (K_p)$$

and $K = K_p/K_m$, where K reflects the resulting transfer process of P from M to P-μE

$$P\text{-}\mu E + M\cdot P \leftrightarrow P\text{-}\mu E\cdot P + M$$

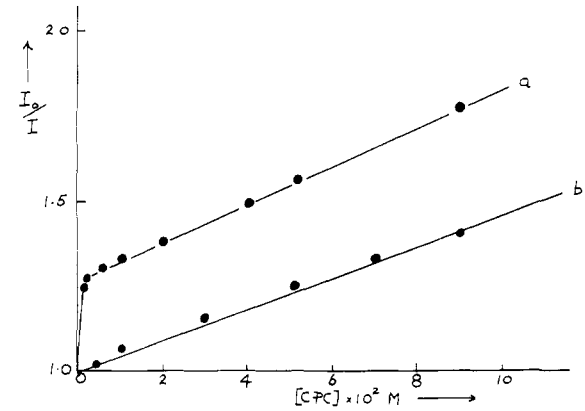

Figure 2. Fluorescence quenching of pyrene in (a) 0.01 M CTAB–P-μE and (b) 0.01 M CPC–P-μE, by CPC. I_0/I is the ratio of fluorescence intensity in the absence of CPC to that with CPC.

The observed linear static quenching of P in the CPC–P-μE is in agreement with this explanation and is entirely due to the partioning of P between the P-μE particles and CPC micelles coexisting in solution. The equilibrium constant derived from the slope is equal in magnitude to that obtained for the CTAB–P-μE system, i.e., $K = 450$ M^{-1}.

Excimer Formation in CTAB- and CPC–P-μE. The fluorescence spectrum of 1.0×10^{-3} M P in 0.01 M CTAB–P-μE obtained by front surface excitation (337 nm) shows a weak excimer emission, and the ratio of the intensity of the excimer (47 nm) to that of the monomer (394 nm) increases with increasing pyrene concentration.

The fluorescence decay of the monomer was found to be nonexponential; however, a good fit is obtained when a double exponential function is used. On the other hand, on monitoring the excimer emission at 500 nm, a rise time (~50 ns) for the maximum emission is observed. This is consistent with the previously reported partitioning for P between the surfactant layer of the P-μE particle and the polymerized core. Therefore it would seem reasonable to attribute the excimer emission to P located in the outer surfactant region which resembles the micelle in many of its properties. The fact that the excimer emission is significantly weaker than that observed in CTAB micelles is explicable in terms of the strong partitioning of P (~75%) in favor of the polymerized core, where the microviscosity is tremendously high and diffusional excimer formation is greatly restricted.

Steady-state fluorescence measurements were also obtained for 1.0×10^{-3} M and 2.0×10^{-3} M P in 0.01 M CPC–P-μE. The observed excimer emission is weaker than that observed in CTAB–P-μE (Table I). The time dependence of the monomer fluorescence decay was first fitted with a sum of two exponential functions. However, in direct contrast to the CTAB–P-μE system, no growth of excimer emission was observed. The excimer emission attained its maximum instantaneously occurring within the laser pulse (~2 nm pulse width). Furthermore, the decay of the excimer emission also followed a double exponential function.

In the CPC polymerized system, no excimer emission would be expected from P located in the surfactant layer, since P* produced in this region would be instantaneously deactivated by the pyridinium head groups of the CPC surfactant located at the surface.

In the polymerized core, due to the large microviscosity one would expect translational motion of solubilized P to be insignificant, if not absent. Also, there will be a large steric hindrance for two P molecules found in close proximity at the time of excitation to achieve the proper orientation necessary for forming the very specific parallel sandwich type configuration deemed essential for excimer formation. All other configurations will probably lead to fluorescence quenching, as the decreased lifetime of the monomer with increasing P would indicate. The observed weak excimer emission is therefore attributed to directly excited preoriented ground-state dimers of P solubilized in the polymerized

Table I. Excimer Formation Data for the Various Aggregated Systems

	[P]	I_E(480 nm)/ I_M(394 nm)	monomer $\tau_1(\alpha)$	monomer $\tau_2(1-\alpha)$	excimer $\tau_1(\alpha)$	excimer $\tau_2(1-\alpha)$
0.01 M CTAB	1.0×10^{-3}	3.24	19 (1.0)		60 (1.0)	
0.1 M CTAB-P-μE	1.0×10^{-3}	0.18	100 (0.7)	400 (0.3)		
	2.0×10^{-3}	0.40				
0.01 M CPC-P-μE	1.0×10^{-3}	0.12	100 (0.55)	400 (0.45)[a]		
			67 (0.75)*	400 (0.25)[b]		
	2.0×10^{-3}	0.3	100 (0.66)	286 (0.45)	67 (0.75)	286 (0.25)
			20 (0.75)*	222 (0.25)*		

[a] Lifetime measurements obtained with low-intensity PRA, N_2 laser. [b] Lifetime measurements obtained with Lambda Physik laser (high intensity).

Table II. Lifetimes and Relative Yields of Fluorescence for 1.0×10^{-5} M P in the Various Aggregate Systems Under Oxygenated, Air-Equilibrated, and Nitrogenated Conditions[a]

	N_2		air		O_2	
	I_F	τ, ns	I_F	τ, ns	I_F	τ, ns
0.01 M CTAB	0.53	1.70	0.36	116	0.16	53
0.01 M CTAB-P-μE	1.00	260	0.86	180	0.68	150
		425		425		320
0.01 M CPC-P-μE	0.88	445	1.79	435	0.64	200
						400

[a] Excitation wavelength used is 337 nm. The fluorescence intensity at 394 nm is taken as measure of relative yield.

domain of the P-μE particle. Steady-state and lifetime data for P excimer formation in the various systems are presented in Table I for purposes of comparison.

It is important to note that at high concentrations of P, where the local concentration in the polymerized structure is ≥ 0.1 M, that excited singlet–excited singlets, S_1–S_1 interaction becomes noticeable when high energy laser is used. This is apparent from the lifetime data for 1.0×10^{-3} and 2.0×10^{-3} M P in 0.01 M CPC–P-μE obtained with two lasers of different energy outputs: (a) excimer laser (10 mJ/pulse—pulse width ~6 ns) and (b) nitrogen laser (50 μJ/pulse—pulse width ~0.2 ns).

Another important difference between the CTAB micelle and CTAB–P-μE is with regard to its solubilization power. It is found[3] that a solution of 0.01 M CTAB–P-μE possesses about twice the solubilization capacity of 0.01 M CTAB for pyrene P.

Accessibility of P to Oxygen and Water Soluble Quenchers. The results of steady-state fluorescence measurements and lifetime data for 1.0×10^{-5} M P solubilized in 0.01 M CTAB, CTAB–, and CPC–PμE are given in Table II. The fluorescence intensities (394 nm) are normalized to that observed in the CTAB–P-μE system. Two points are worth making here. First, the fluorescence yield of P in CPC–P-μE is decreased only to 88% of that observed in CTAB–P-μE, suggesting that only about 12% of P* is quenched by CPC (under these conditions, no fluorescence could be detected for 1.0×10^{-5} M P in 0.01 M CPC). Secondly, the accessibility of P* to O_2 in the aqueous phase is significantly diminished in the polymerized μE systems. This effect is reflected in both the fluorescence intensities as well as the lifetime data.

Earlier studies[9] showed that nitromethane was found to be very effective in quenching the fluorescence of P in CTAB micelles. Steady-state and lifetime measurements yielded bimolecular quenching rate constants in homogeneous solutions and micelles which are close to the diffusion-controlled limit of 5.0×10^9 M^{-1} s^{-1}. On the other hand, this quencher is very inefficient in quenching the fluorescence of P incorporated into CTAB– or CPC–P-μE. An upper limit for an apparent bimolecular rate constant could be set at $< 6 \times 10^7$ M^{-1} s^{-1}. This low rate is due to the rigid nature of the pyrene environment in the PμE.

Quenching of the triplet state of P (monitored at 415 mn) by O_2 was also investigated in the various systems. For an air-equilibrated solution of 5.0×10^{-5} M P in 0.01 CTAB, an exponential decay with a lifetime of 2.1 μs was measured. By use

(9) S. G. Wallace and J. K. Thomas, *Radiat. Res.*, **54**, 49 (1973).

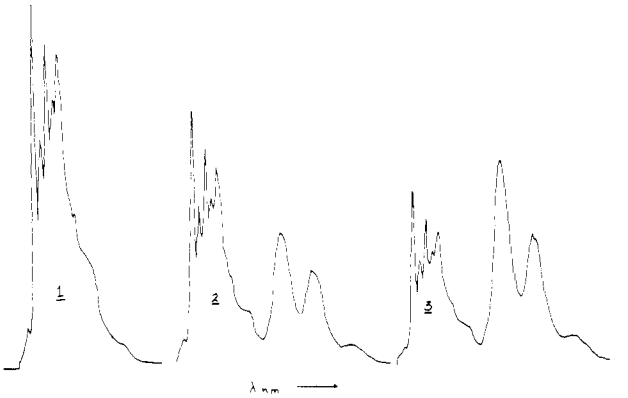

Figure 3. Fluorescence emission spectra of pyrene (P) and perylene (Pe) in 0.01 M CTAB–P-μE: (1) 10^{-5} M pyrene; (2) 10^{-5} P, 10^{-5} M Pe; and (3) 10^{-5} M P, 2.5×10^{-5} M Pe. Excitation wavelength, 337 nm.

of the oxygen concentration in water (2.5×10^{-4} M),[10] a bimolecular quenching rate constant of 2×10^9 M^{-1} s^{-1} is calculated. In the case of CTAB- and CPC-polymerized systems, two effects were noted: first, the observed yield of P^T, triplets was reduced to 20%, and secondly, the lifetime of P^T was ~6 times longer than that observed in CTAB micellar solution.

From the results presented above, it can be concluded that while P solubilized in CTAB micelles is quite accessible to water soluble quenchers, when solubilized in the polymerized systems, either CPC–P-μE or CTAB–P-μE, it becomes greatly inaccessible to species present in the aqueous phase. Thus it would seem that the P-μE systems offer a protective environment for P.

Energy Transfer between Pyrene P, and Perylene Pe, in CPC–P-μE System. The substantial overlap between the emission of P and absorption of Pe predicts an efficient Förster-type dipole–dipole resonance energy transfer from the excited state of P to the ground state of Pe. The critical transfer distance R_0, has already been determined and found to be 35 Å.[11,12]

Figure 3 shows the total emission spectrum of 1.0×10^{-5} M P in 0.01 M CPC–P-μE, and with added Pe (10^{-5} to 10^{-4} M), obtained in a steady-state experiment where P is preferentially excited at 335 nm. Evidence for an efficient energy transfer in this system is noted in the effective quenching of the fluorescence of P and the concomitant appearance of the enhanced Pe emission.

The time dependence of P* fluorescence decay in the presence of varying [Pe] is seen to deviate markedly from exponentiality as predicted from Förster's theory of resonance energy transfer under conditions where the random distribution of distances between the donor and acceptor remain effectively unperturbed during the lifetime of excited donor (i.e., $(4D\tau)^{1/2} \ll R$, where D is the sum of donor and acceptor diffusion coefficients and τ is the lifetime of the excited state of the donor).

According to Förster's theory for an isolated pair of a donor and an acceptor separated by a distance R, the rate of energy

(10) "Handbook of Chemistry and Physics", 49th ed., p B225.
(11) I. Berlman, "Energy Transfer Parameters of Aromatic Compounds", Academic Press, New York, 1973.
(12) N. Mataga, H. Obashi, and T. Okada, *J. Phys. Chem.*, **73**, 370 (1969).

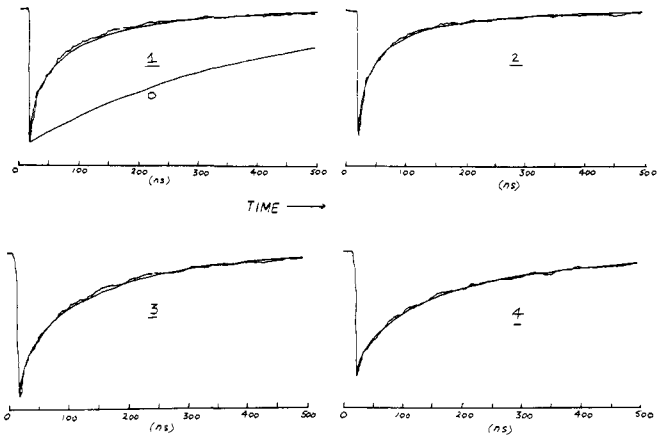

Figure 4. Rate of decay of pyrene fluorescence in CPC–P-μE with various concentrations of perylene; coarse curve, experimental data; smooth curve, calculated curve according to eq 1; [pyrene]: 10^{-5} M; [perylene]: (1) 0 and 10^{-4} M; (2) 2×10^{-4} M; (3) 5.0×10^{-5} M; and (4) 2.5×10^{-5} M.

Table III. Energy Transfer Parameters for 1.0×10^{-5} M P in 0.01 M CPC-P-μE with Pe as an Acceptor

[Pe] $\times 10^4$		R, Å	
		exptl	theor
0.10	0.50	53	60
0.25	0.85	45	45
0.50	1.50	37	35
1.00	2.25	32	28

transfer from the excited donor to the acceptor is given by $k = k_1(R_0/R)^6$, where k_1 is the sum of all first-order processes leading to the deactivation of excited donor in the absence of the acceptor (i.e., $k_1 = 1/\tau$).

In a rigid matrix where the donor and acceptor molecules are randomly and statically distributed, the decay of the fluorescence of the donor excited state would therefore be given by

$$I_F(t) = I_F(t = 0) \exp\left[-\left(k_1 t + \sum_{n=1}^{N}\left(\frac{R_0}{R}\right)^6 k_1 t\right)\right]$$

where N is the number of acceptor molecules surrounding the donor. If N tends to infinity, the decay of an excited donor molecule can be represented by

$$I_F(t) = I_F(t = 0) \exp[-(k_1 t + \beta(k_1 t)^{1/2})] \qquad (1)$$

where $\beta = \pi^{1/2}[\mathrm{Pe}]/[\mathrm{Pe}]_0$, and [Pe] is the total concentration of Pe given by $^3/_4\pi R^3 N_0$, and $[\mathrm{Pe}]_0$ is the critical transfer concentration of Pe. There β would then be given by $\beta = \pi^{1/2}(R_0/R)^3$.

Analysis of the fluorescence decay of P* in the presence of various [Pe] according to eq 1 is shown in Figure 4, where the dotted curves are computer fits to the experimental decay curves (solid). The best-fit values of β for the different concentrations of [Pe] are given in Table III. From these values and the known R_0 (35 Å), one can estimate the average intermolecular distance (R) between P and Pe in the polymerized phase of the P-μE particle at different [Pe]. Inspection of Table III shows good agreement between the experimentally determined R and that calculated based on the effective concentration of Pe in the polymerized particles which gives support to the method of analysis just described. It also demonstrates the rigidity of the polymerized core of the p-μE particle which prevents trapped molecules from diffusing within the system during the measurement.

Laser-Induced Electron Transfer Reactions in CPC–P-μE. Photoinduced electron transfer reactions have been extensively studied in homogeneous fluid solutions, but considerably less attention has been given to the study of these processes under conditions which more closely resemble that which exist in vivo. It is conceivable that the parameters of these reactions can be altered by factors such as constraints upon diffusion of the reacting species as well as their relative orientation ion and microenvironment.

One cannot restrict mechanisms of electron transfer reactions to those only determined by diffusion. Recently, long-range electron tunneling has been suggested as a mechanism for electron transfer in chemical and biological systems. A simplified discussion of the theory is presented below leading to an expression for the decay of excited probe involved in an electron tunneling quenching process.[13]

The driving force for the long range electron tunneling is the finite interaction between the reacting species. The energy of this interaction is proportional to the overlap of the wave functions of the two reactants. Since these wave functions decay approximately exponentially with distance r, their overlap and the probability of tunneling also decreases with the distance between the interacting species in an exponential manner. According to a simplified model,[14,15] the rate constant for the electron tunneling process is given by $k = Fve^{-r/a}$, where F is an inefficiency factor, which is strongly related to the electron affinity of the acceptor molecule, ranging from 10^4 to 10^{-16} in magnitude, v is the collision frequency of the transferring electron with the barrier—equal to the characteristic frequency of the motion of the electrons in atoms (10^{14}–10^{15} s^{-1}), and a is a measure of the binding energy of the electron given by $2\hbar/(2mV)^{1/2}$, where $\hbar$ is Planck's constant, m is the mass of the electron, V is equivalent to the ionization potential of the donor molecule, and r is the transfer distance.

It is important to note here that k decreases exponentially as the mass of the transferring particle increases, and hence the most effective tunneling transition is expected to occur in electron transfer reactions, which involve the lightest of all chemical particles, electrons.

The probability that the excited state of a fluorescence probe P* will survive at time t is given by

$$I_F(t)/I_F(t = 0) = \exp[-(k_1 t + \sum_{i=1}^{N} k(\gamma_i)t)]$$

where $k(\gamma_i)$ is the rate constant for the electron tunneling process when P* and the quencher molecule are separated by a distance r_i, N is the total number of quenchers in the system, and k_1 is the first-order rate of decay of P* in the absence of quencher Q.

For a random distribution of P* and Q, the P* survival probability takes the form

$$\frac{I_F(t)}{I_F(t = 0)} = \exp\left[-\left(k_1 t + \frac{4}{3}\pi a^3 N_Q \ln^3 Fvt\right)\right] \qquad (2)$$

where N_Q is the number of quencher molecules per Å^3, and the tunneling distance in time t is given by (a ln Fvt).

Decay of Laser-Produced Excited State of Pyrene in the Presence of Electron Donors and Acceptors in CPC–P-μE Systems. Two different types of electron transfer quenching reactions were scrutinized in CPC–P-μE. In one case dimethylaniline (DMA) was used as an electron donor quencher, where the electron is transferred from the highest occupied orbital of DMA to the lowest singlet excited state of P. In another, nitrobenzene (NB) was utilized as an electron acceptor where in this case an electron is ejected from P* into the lowest unoccupied orbital of NB. Unfortunately, we could not use DMA as a quencher since it was found that it forms a ground state complex with CPC head groups, which complicates analysis of the kinetic data. Therefore quenching studies are restricted in the analysis of P* decay in the presence of NB. Analysis of steady-state fluorescence measurements using this quencher is projected to be rather difficult to interpret since NB absorbs strongly at the excitation wavelength (337 nm).

In the absence of added quencher, P* decays exponentially with a time constant of 2.5×10^6 s^{-1}. Because of the nature of the

(13) N. Sutin, *Acc. Chem. Res.*, **15**, 275 (1982).
(14) J. Ulstrup and J. Jortner, *J. Chem. Phys.*, **63**, 4358 (1975); **64**, 4860 (1969).
(15) J. R. Miller and J. V. Beitz, "Proceeding of Sixth International Congress of Radiation Research, 1979, p 301.

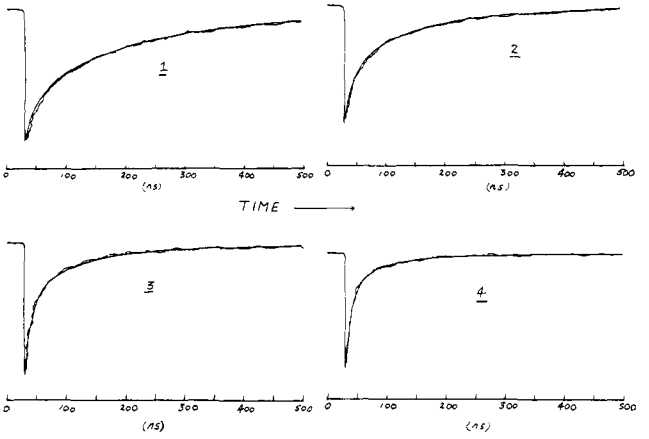

Figure 5. Rate of decay of pyrene fluorescence in CPC–P-μE in the presence of nitrobenzene; [pyrene] = 10^{-5} M; [nitrobenzene]: (1) 10^{-3} M; (2) 2.5×10^{-3} M; (3) 5×10^{-3} M; and (4) 10^{-2} M. Coarse curve, experimental data; smooth curve, calculated curve according to eq 2.

Table IV. Kinetic Parameters for Quenching the Fluorescence of 1.0×10^{-6} M P in 0.01 M CPC-P-μE by Nitrobenzene, NB

$[Q] \times 10^3$	A^a	$k_1 \times 10^{-6}$ s^{-1}	$Ev \times 10^{-10}$ s^{-1}
0	0	2.52	0
1.0	0.002	2.52	1.0
2.5	0.0035	2.52	1.0
5.0	0.005	2.52	1.0
7.5	0.0062	2.52	1.0

$^a A = {}^4/_3\pi a^3 N_Q$.

pyridinium head groups as effective quenchers of P*, it can be safely presumed that this fluorescence is exclusively emanating from P* intercalated in the polymerized matrix of pμE. However, in the presence of NB at a quencher occupancy level greater than one hundred, where the statistical distribution of quenchers among the p-μE particles becomes unimportant, the decay of the fluorescence of P* is distinctly nonexponential, and attempts to fit it with a double exponential function proved unsuccessful. The apparent dynamic quenching of P* cannot be explained by a diffusional encounter mechanism between P* and Q within the sphere of the polymerized latex particle, since it has already been established that movement of entrapped species is greatly restricted if not absent within the time of the experiment.

On the other hand, excellent fits to the fluorescence decay curves (Figure 5) were obtained with the tunneling equation (2) by maintaining the parameters (Fv) and k_1 fixed and varying (${}^4/_3\pi a^3 N_Q$). Optimal values of these parameters are displayed in Table IV. Attention should be given to the fact that the parameter (${}^4/_3\pi a^3 N_p$) was found to increase with quencher concentration, but a linear relationship was not found according to the theoretical prediction. This could be a consequence of a nonuniform and complex distribution of quencher between the polymerized phase, the surfactant layer, and the aqueous phase. Nonetheless, the goodness of fit between the experimental decay curves at different concentrations of quencher and the computer-generated curves using eq 2 lend credence to the electron tunneling kinetic model presented above.

Conclusion

Polymerized microemulsion systems add yet another attractive parameter to the use of micelles and microemulsions in photochemistry, namely the possibility of arranging reactants into two well-defined regions of space in the same molecular assembly. Reactants may be in the surfactant coating, where the dominant kinetic event is diffusion, or the reactants may be on the polymerized core, where the dominant kinetic events are Förster type energy transfer and tunneling type electron transfer.

Registry No. CTAB, 57-09-0; CPC, 123-03-5; P, 129-00-0; Pe, 198-55-0; NB, 98-95-3; divinylbenzene–styrene copolymer, 9003-70-7.

Variable-Temperature Photoelectron Spectral Study of 1,3-Dithiol-2-one and 4,5-Disubstituted 1,3-Dithiol-2-ones. Thermal Generation of 1,2-Dithiete, 3,4-Disubstituted 1,2-Dithietes, and Dialkyl Tetrathiooxalates[1]

Reinhard Schulz,[2a] Armin Schweig,*[2a] Klaus Hartke,[2b] and Joachim Köster[2b]

Contribution from the Fachbereich Physikalische Chemie and the Institut für Pharmazeutische Chemie, Universität Marburg, D-3550 Marburg, West Germany. *Received December 27, 1982*

Abstract: The thermal fragmentation of 1,3-dithiol-2-one, its 4,5-dimethyl, dicyano, monocyclic 4,5-dialkylthio ($R^4 = R^5 = SCH_3$, SC_2H_5, $SCH(CH_3)_2$), and bicyclic alkylthio derivatives ($R^{4,5} = SCH_2S$, $S(CH_2)_2S$, $S(CH_2)_3S$) was investigated by variable-temperature photoelectron spectroscopy and in part by the matrix-isolation technique and infrared spectroscopy. The photoelectron spectra of the reactive intermediates 1,2-dithiete, 3,4-dimethyl-1,2-dithiete, and diethyl tetrathiooxalate are presented and interpreted. The new reactive species are unambiguously identified by photoelectron spectral and quantum chemical means. In addition, the photoelectron spectra of the stable (i.e., isolable at room temperature) compounds 3,4-bis(trifluoromethyl)-1,2-dithiete and dimethyl tetrathiooxalate are discussed. The influence of substituents on the relative stabilities of the 1,2-dithiete vs. the 1,2-dithione structures is studied using the MNDO method. The theoretical as well as the experimental results show that 1,2-dithiete and 3,4-dimethyl-1,2-dithiete are thermodynamically favored above their 1,2-dithione counterparts.

Variable-temperature photoelectron spectroscopy (VTPES) is a valuable tool for generating and observing reactive species in thermal reactions.[3,4] Our present experimental setup allows for the detection of reactive intermediates having a lifetime of ca.

0002-7863/83/1505-4519$01.50/0